Contribution from the Evans and McPherson Chemical Laboratories,
The Ohio State University, Columbus, Ohio 43210

Structural Dependence of an Electron-Transfer Process: Nature of the Products of One-Electron Oxidation of the Lacunar Cyclidene Complexes of Nickel(II) and Cobalt(II)

Madhav Y. Chavan, Thomas J. Meade, Daryle H. Busch,* and Theodore Kuwana*

The lacunar and related unbridged macrocyclic cyclidene complexes of nickel(II) and cobalt(II), $[M^{II}L]^{2+}$, were electrochemically oxidized to generate the corresponding $[ML]^{3+}$ complexes in solution. The nature of the $[ML]^{3+}$ complexes was studied by using ESR, UV–visible spectroscopy, and magnetic moment measurements. The dependence of the natures of these $[ML]^{3+}$ species on the strength and extent of axial ligation has been observed. The axial ligation is dependent, in turn, on the size of the lacuna. The results of ESR and electronic spectroscopy at various temperatures indicate that the unpaired electron in the $[NiL]^{3+}$ resides on the metal at lower temperatures in those cases where a six-coordinate complex can be formed by the addition of two monodentate axial acetonitrile ligands. The resulting complexes contain nickel(III). In contrast, at higher temperatures and in those cases where a six-coordinate complex cannot be formed, the unpaired electron resides on the macrocyclic ligand and the resulting complex contains nickel(II). In this second situation the ligand has been oxidized, $[Ni^{II}(L^{+}\cdot)]^{3+}$. Electronic spectral studies and magnetic moment measurements on the oxidized cobalt complexes $[CoL]^{3+}$ indicate that ordinary six-coordinate diamagnetic cobalt(III) complexes exist when it is possible for two monodentate axial ligands to bind to the cobalt. However, in the contrasting case where the size of the lacunae prevents coordination of the sixth ligand, paramagentic species having two unpaired electrons are formed. These paramagnetic species are believed to involve low-spin cobalt(II) ions and ligand radicals formed by oxidation at the ligand rather than at the metal center. In these systems it is concluded that the oxidation product of the electron-transfer process is determined by the extent of axial ligation. It follows that changes in axial ligation lead to intramolecular electron transfer.

Introduction

A new family of so-called lacunar *cyclidene* ligands has recently been developed[1-4] for the purpose of elucidating the interactions between dioxygen and complexes of cobalt(II) and iron(II).[5-7] These remarkable new substances provide the first examples of non-porphyrin iron complexes capable of reversibly binding dioxygen at room temperature. Further, the cobalt(II) derivatives show exceptionally high dioxygen affinities and unusual resistance to autoxidation even in aqueous solutions. Lacunar complexes are generally characterized by a permanent void, or lacuna, in the vicinity of one of the metal atom coordination sites. The lacunar cyclidene complexes are represented in Figure 1, where the R^1 group provides the roof to the lacuna and the ligands in structures I and II contain 16-membered and 15-membered parent *cyclidene* macrocycles, respectively.

Many studies have shown that the most fundamental properties of dioxygen carriers, including their dioxygen affinities and their tendencies to be destroyed by autoxidation, are sensitive to the oxidation–reduction behaviors of the metal complexes. In view of the unusual promise of the lacunar cyclidene complexes as dioxygen carriers, an exploration of their oxidation–reduction behavior is of considerable interest.

Since nickel(II) served as the template during ligand synthesis, the complexes of this metal ion are also available for study. As reported earlier,[1,2] the nickel(II) lacunar complexes, $[Ni^{II}L]^{2+}$, where L = ligand, show a reversible one-electron oxidation to a species of the general formula $[NiL]^{3+}$. The potential for this oxidation varies with the substituents R^2 and R^3 that are positioned at the openings to the lacuna (Figure 1). A similar substituent effect for the first one-electron-oxidation process has been observed for the corresponding iron(II) complexes. In both cases, the

oxidation potential for the first process shifts to more positive values when electron-withdrawing substituents are placed in the R^3 positions.[1,2,4]

The equlilibrium constants for dioxygen binding (K_{O_2}) for the cobalt(II) and iron(II) lacunar complexes are sensitive to the length and structure of the bridging group R^1 and to the nature of the substituent R^3. The equilibrium constant decreases as the length of the bridge decreases and when the electron-withdrawing character of R^3 increases.[4,8]

An important link to redox behavior arises from the fact that dioxygen binding effectively constitutes oxidation of the metal ion. In this report we deal with the nature of the product of electrochemical one-electron oxidation of the lacunar cyclidene nickel(II) and cobalt(II) complexes. Attention is focused on the relationships associated with alterations in the bridging group R^1. For the purpose of the study, R^1 is either a bridging polymethylene group or, for meaningful contrast, a pair of nonbridging methyl groups, although other moieties have been incorporated into this structural component. Structures are further restricted in this study to the cases where $R^2 = R^3 = CH_3$. The nickel complexes were studied in acetonitrile solution, while both acetonitrile and acetone solvents were used in studies on the cobalt complexes. Tetra-*n*-butylammonium tetrafluoroborate ($(TBA)BF_4$, 0.1 M) served as supporting electrolyte in both solvents, and measurements were made under dry nitrogen with the cell in a controlled-atmosphere enclosure.

Results and Discussion

Electrochemical Studies. Figure 2 illustrates the cyclic voltammograms for the oxidation of the nickel complexes with the 16-membered lacunar cyclidene ligands and the related unbridged ligand $[Ni(16L)]^{2+/3+}$ in acetonitrile at different sweep rates. This oxidation process is reversible for all of the nickel complexes with these ligands, as evidenced by a common 60-mV separation between the cathodic and anodic peak potentials (ΔE_p). The corresponding lacunar cobalt complexes ($[Co(16L)]^{2+/3+}$) also exhibit scan-rate-independent, reversible cyclic voltammogrms when measured under the same conditions ($\Delta E_p = 60–70$ mV) (Figure 3). However, the unbridged cobalt complex displays a scan-rate dependence with ΔE_p ranging from 80 mV at a scan rate of 0.02 V/s to 150 mV at 0.2 V/s. In acetone solutions containing 0.1

(1) Busch, D. H.; Olszanski, D. J.; Stevens, J. C.; Schammel, W. P.; Kojima, M.; Herron, N.; Zimmer, L. L.; Holter, K. A.; Mocak, J. *J. Am. Chem. Soc.* **1981**, *103*, 1472.
(2) Korybut-Daszkiewicz, B.; Kojima, M.; Cameron, J. H.; Herron, N.; Chavan, M. Y.; Jircitano, A. J.; Coltrain, B. K.; Neer, G. L.; Alcock, N. W; Busch, D. H. *Inorg. Chem.* **1984**, *23*, 903.
(3) Stevens, J. C.; Jackson, P. J.; Schammel, W. P.; Christoph, G. G.; Busch, D. H. *J. Am. Chem. Soc.* **1980**, *102*, 3283.
(4) Herron, N.; Zimmer, L. L.; Grzybowski, J. J.; Olszanski, D. J.; Jackels, S. C.; Callahan, R. W.; Christoph, G. G.; Busch, D. H., submitted for publication.
(5) Stevens, J. C.; Busch, D. H. *J. Am. Chem. Soc.* **1980**, *102*, 3285.
(6) Herron, N.; Busch, D. H. *J. Am. Chem. Soc.* **1981**, *103*, 1236.
(7) Herron, N.; Cameron, J. H.; Neer, G. L.; Busch, D. H. *J. Am. Chem. Soc.* **1982**, *105*, 298.

(8) (a) Holter, K. A. Ph.D. Thesis, The Ohio State University, 1978. (b) Stevens, J. C. Ph.D. Thesis, The Ohio State University, 1979. (c) Jackson, P. J. Ph.D. Thesis, The Ohio State University, 1981.
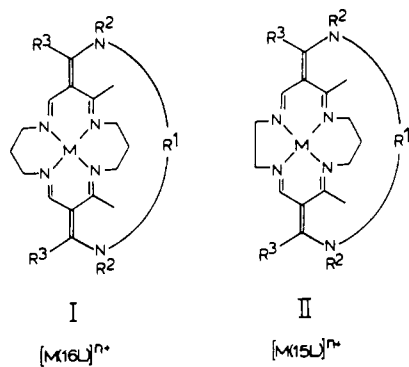
Figure 1. Lacunar complexes studied: $R^1 = (CH_2)_{3-8,12}$, $(CH_3)_2$; $R^2 = CH_3$; $R^3 = CH_3$, C_6H_5.
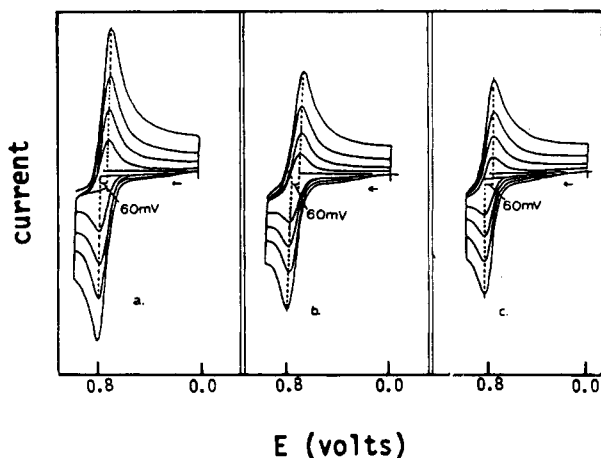
Figure 2. Cyclic voltammograms of the $2+/3+$ redox couple of the nickel(II) complexes with varied R^1 substituent ($R^2 = R^3 = CH_3$), recorded inside the dry atmosphere glovebox at a Pt-disk working electrode, $Ag/AgNO_3$ (0.1 M in acetonitrile) reference, Pt-wire auxiliary electrode. Scan rates: 20, 50, 100, 200 mV/s. About 1 mM acetonitrile solution with 0.1 M (TBA)BF$_4$ supporting electrolyte was used: (a) $R^1 = (CH_3)_2$ (unbridged); (b) $R^1 = (CH_2)_7$; (c) $R^1 = (CH_2)_3$.

Table I. Half-Wave Potentials for the First Oxidation of Nickel(II) and Cobalt(II) Lacunar Complexes (Structures I and II, Figure 1) in Acetonitrile (0.1 M (TBA)BF$_4$)[a]

	$E_{1/2}$,[b] V			
R^1	[Ni-(16L)]$^{2+/3+}$	[Ni-(15L)]$^{2+/3+}$	[Co-(16L)]$^{2+/3+}$	[Co-(15L)]$^{2+/3+}$
$(CH_3)_2$	0.74*	0.58[c]	−0.15	−0.20
$(CH_2)_{12}$	0.74	0.53	...	
$(CH_2)_8$	0.77	0.65	0.05*	0.007
$(CH_2)_7$	0.78	...	0.08*	0.12
$(CH_2)_6$	0.76	0.68	0.20	0.21
$(CH_2)_5$	0.78	...	0.28	
$(CH_2)_4$	0.79		0.34	
$(CH_2)_3$	0.79		0.34	

[a] $R^2 = R^3 = CH_3$; R^1 is varied. [b] Measured by using rotating Pt-disk electrode vs. $Ag/AgNO_3$ 0.1 M in acetonitrile. Values for [Ni-(16L)]$^{2+/3+}$ and [Co(16L)]$^{2+/3+}$, except for those identified by asterisks, were first reported in ref 8. These values have been verified and, in a few cases, corrected. [c] Two reversible redox waves separated by ~80 mV are present in the cyclic voltammograms.

M (TBA)BF$_4$ (Figure 4), all of the cobalt complexes show reversible $2+/3+$ oxidation reactions that are independent of the R^1 group and of the scan rates employed (0.02–0.05 V/s). Mechanistic considerations that rationalize the somewhat varied behavior of cobalt cyclidene complexes are discussed elsewhere.[9]

The response of the electrochemical oxidation process to changes in bridge length (R^1) is quite similar for nickel and iron but it
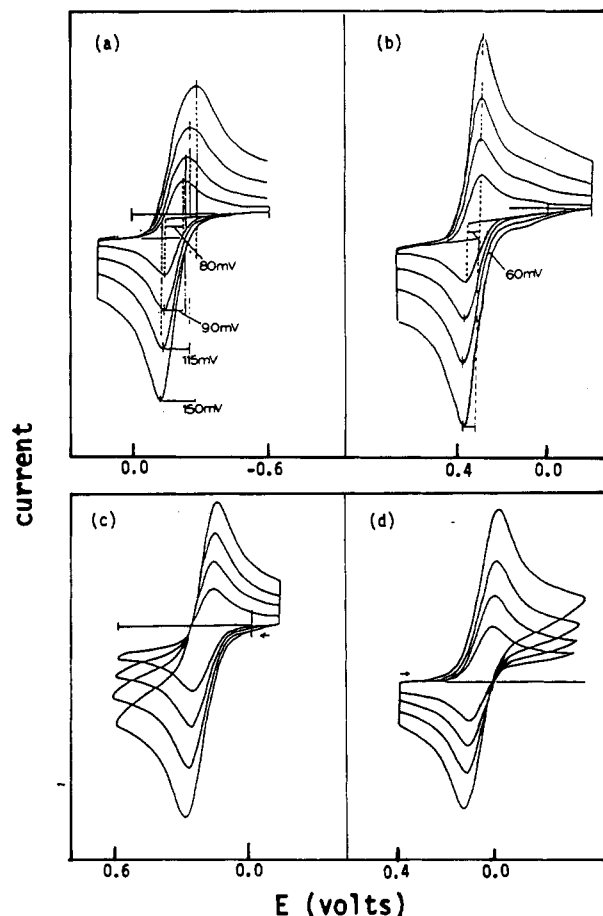
Figure 3. Cyclic voltammograms of the $2+/3+$ redox couple of the [Co(16L)]$^{2+}$ complexes with varied R^1 substituent ($R^2 = R^3 = CH_3$), recorded inside the dry nitrogen atmosphere glovebox at a Pt-disk working electrode, $Ag/AgNO_3$ (0.1 M in acetonitrile) reference, Pt-wire auxiliary electrode. Scan rates: 20, 50, 100, 200 mV/s. A bulk solution of [Co(16L)]$^{3+}$ and about 1 mM acetonitrile solution with 0.1 M (TBA)BF$_4$ supporting electrolyte was used: (a) $R^1 = (CH_3)_2$ (unbridged); (b) $R^1 = (CH_2)_4$; (c) $R^1 = (CH_2)_6$; (d) $R^1 = (CH_2)_8$.
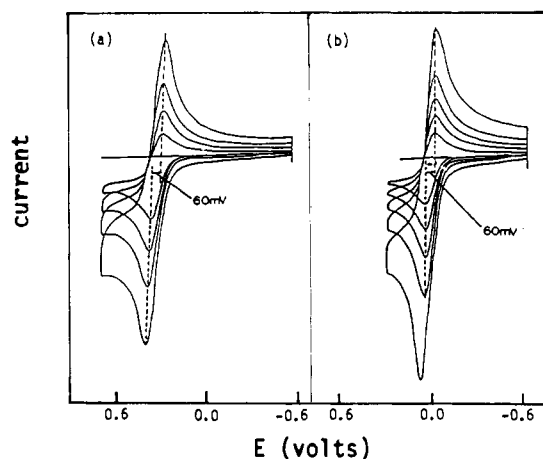
Figure 4. Cyclic voltammograms of the $2+/3+$ redox couple of the complexes with varied R^1 substituent ($R^2 = R^3 = CH_3$), recorded inside the dry nitrogen atmosphere glovebox at a Pt-disk working electrode, $Ag/AgNO_3$ (0.1 M in acetonitrile) reference, Pt-wire auxiliary electrode. Scan rates: 20, 50, 100, 200 (and 500 for part b) mV/s. About 1 mM acetone solution with 0.1 M (TBA)BF$_4$ supporting electrolyte was used: (a) $R^1 = (CH_2)_6$; (b) $R^1 = (CH_3)_2$ (unbridged).

is dramatically different for cobalt. This is shown in the graphs of Figure 5. The data for the nickel and cobalt complexes are reported in Table I; for the iron data, see ref 4.

The first oxidation potential for the nickel and iron complexes is insensitive to changes in the length of the polymethylene bridging

---

(9) Chavan, M. Y.; Busch, D. H.; Kuwana, T., manuscript in preparation.
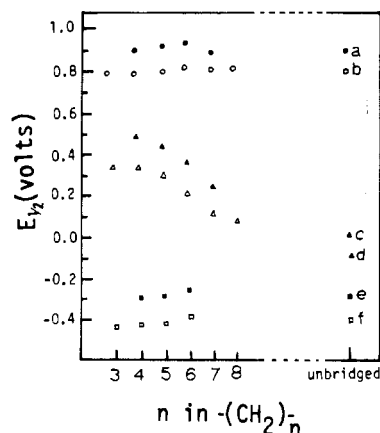
Figure 5. Relationship between $E_{1/2}$ (measured by rotating Pt electrode technique[4,8c] vs. Ag/AgNO$_3$ 0.1 M) of the [M(L)]$^{2+/3+}$ redox process in acetonitrile (0.1 M (TBA)BF$_4$) and the number of carbon atoms in the bridging group R^1: (a) M = Ni, R^3 = C$_6$H$_5$, R^2 = CH$_3$; (b) M = Ni, R^3 = R^2 = CH$_3$; (c) M = Co, R^3 = C$_6$H$_5$, R^2 = CH$_3$; (d) M = Co, R^3 = R^2 = CH$_3$; (e) M = Fe, R^3 = C$_6$H$_5$, R^2 = CH$_3$; (f) M = Fe, R^3 = R^2 = CH$_3$ (16-membered macrocycles).

group R^1. The potentials for these processes vary with the R^3 group, shifting ~100 mV in the positive direction when a methyl group is replaced by a phenyl group. On the other hand, the first oxidation potential of the cobalt(II) complexes depends strongly on the length of the bridging group. When one proceeds from an unbridged structure through decreasing bridge lengths to the shortest bridge (R^1 = (CH$_2$)$_3$), the potential spans a range of nearly 500 mV, going from −0.15 to +0.34 V. This change in the bridging group is equivalent to going from an infinitely large lacuna (unbridged case, R^1 = (CH$_3$)$_2$) to a very restrictive lacuna having only a trimethylene bridge. Other studies have shown that the latter cavity is too small to accomodate even such small ligands as O$_2$ and CO.[10] Clearly the shorter bridges do not favor the higher oxidation state ([CoL]$^{3+}$). We prefer NOT to refer to the metal ion oxidation state for reasons that will become clear as the discussion proceeds. The investigation of the nature of the oxidation products ([NiL]$^{3+}$ and [CoL]$^{3+}$) as a function of bridge length is germane, and that subject is treated in the sections that follow.

The first oxidation potentials for the nickel(II) and cobalt(II) complexes respond differently to changes in macrocyclic ring size. The data in Table I permit a comparison for derivatives of the 15-membered macrocyclic cyclidene and the 16-membered cyclidene. When the macrocyclic cyclidene decreases in size (from 16L to 15L), the potentials for the nickel complexes shift to more negative values by about 100 mV, all else being equal. The same structural change for the cobalt complexes produced only small unsystematic variations in potential.

It has long been known that the Co$^{3+/2+}$ couple is relatively insensitive to the in-plane ligand field strength while it is more sensitive to axial ligand field strength.[11] On the other hand, a ring-size effect has been documented and it might seem surprising that no such effect is seen here. This result is consistent with the earlier conclusion[12] that the largest ring size effects seen for this cobalt couple arise from the release of strain energy when the best fitting metal ion is formed. In view of the relatively rigid cyclidene structure, strain energy contributions are probably small. Therefore, the insensitivity of the cobalt couple to ring size is easily rationalized.

Controlled-potential electrolysis has been applied to demonstrate that the first oxidation processes for the lacunar cyclidene complexes involve a single electron transfer (Table II). The elec-

(10) Herron, N.; Chavan, M. Y.; Busch, D. H. *J. Chem. Soc., Dalton Trans.* **1984**, 1491.
(11) Tait, A. M.; Lovecchio, F. V.; Busch, D. H. *Inorg. Chem.* **1977**, *16*, 2206.
(12) Hung, Y.; Martin, L. Y.; Jackels, S. C.; Tait, A. M.; Busch, D. H. *J. Am. Chem. Soc.* **1977**, *99*, 4029.

Table II. Results of Controlled-Potential Electrolysis of [M^{II}(L)]$^{2+}$ Lacunar Complexes^a

M	R^1	$E_{1/2}$,^{b} V	$E_{applied}$,^{b} V	coulometric data, C expected^c	coulometric data, C measd^d	n
Ni	(CH$_3$)$_2$	0.74	0.90	1.35	1.29	1
	(CH$_2$)$_{12}$	0.74	0.92	1.21	1.30	1
	(CH$_2$)$_8$	0.77	0.94	1.12	1.08	1
	(CH$_2$)$_7$	0.78	0.94	1.72	1.60	1
	(CH$_2$)$_6$	0.76	0.94	2.20	2.21	1
	(CH$_2$)$_4$	0.79	0.94	1.31	1.26	1
	(CH$_2$)$_3$	0.79	0.94	1.15	1.10	1
Co	(CH$_3$)$_2$	−0.15	0.25	2.25	2.32	1
	(CH$_2$)$_8$	0.05	0.50	2.11	2.16	1
	(CH$_2$)$_7$	0.08	0.60	1.86	1.93	1
	(CH$_2$)$_6$	0.20	0.60	1.76	1.66	1
	(CH$_2$)$_4$	0.34	0.60	1.90	1.92	1
	(CH$_2$)$_3$	0.34	0.60	2.34	2.25	1

^{a} M = Co or Ni, R^3 = R^2 = CH$_3$, and R^1 is varied. ^{b} All values except those for R^1 = (CH$_2$)$_3$ and (CH$_2$)$_{12}$ bridged complexes were initially reported in ref 8. These values have been verified and, in a few cases, corrected. Determined from rotating platinum-disk electrode (vs. Ag/AgNO$_3$, 0.1 M) results in acetonitrile with 0.1 M tetra-n-butylammonium fluoroborate as supporting electrolyte. ^{c} Calculated assuming n = 1. ^{d} ±0.05 C.
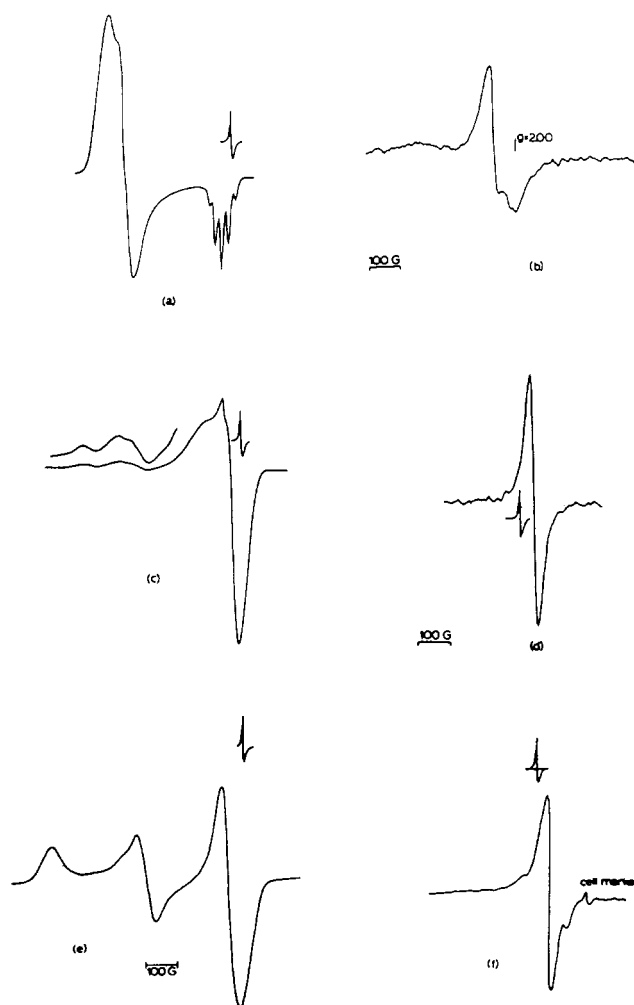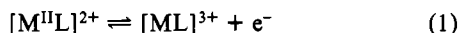

Figure 6. ESR spectra of various electrogenerated [Ni(16L)]$^{3+}$ species in acetonitrile (0.1 M (TBA)BF$_4$) under dry nitrogen recorded at 77 K (a, c, e) and at room temperature (b, d, f) for [Ni(16L)]$^{3+}$ complexes with R^2 = R^3 = CH$_3$ and (a, b) R^1 = (CH$_3$)$_2$ (unbridged), (c, d) R^1 = (CH$_2$)$_6$, and (e, f) R^1 = (CH$_2$)$_3$.

trolyses were carried out in the controlled atmosphere enclosure using 0.1 M (TBA)BF$_4$ solutions in acetonitrile. The diffusion-controlled reversible electrode reaction is properly represented in eq 1. Equation 1 does not consider the axial ligation of the metal

$$[M^{II}L]^{2+} \rightleftharpoons [ML]^{3+} + e^- \qquad (1)$$

ions in the 2+ or the 3+ species, nor does it consider the site of oxidation.

ESR Studies on the Nickel Complexes (0.1 M (TBA)BF$_4$ in Acetonitrile). The ESR spectrum for the oxidation product from electrolysis of the unbridged nickel complex, $[NiL]^{3+}$, is shown in Figure 6a. The data were obtained at 77 K in a dry N$_2$ atmosphere. The spectrum is typical of six-coordinate, tetragonal nickel(III) (low spin d^7),[13] with $g_\perp > g_\parallel$. The parallel signal, $g_\parallel$, is split into a quintet by interaction with the nitrogen atoms ($I = 1$) of two axial acetonitrile ligands. It is not surprising that the ESR spectrum of this complex is poorly resolved at room temperature since the isoelectronic cobalt(II) lacunar complexes do not exhibit well-defined ESR spectra at such temperatures. It is significant that the bridged complex having an octamethylene bridge also gave an ESR spectrum characteristic of low-spin six-coordinate nickel(III) at 77 K.

The strongest contrast is seen by comparison with the complex having the most restricted cavity, the trimethylene derivative. At 77 K the ESR spectrum of this species displays an isotropic signal at $g = 2.00$ (Figure 6e). In addition, this spectrum shows two signals at $g > 2.0$, giving a pattern similar to that reported for low-spin nickel(III) complexes having coordination numbers lower than six. This part of the spectrum resembles those of certain square-planar nickel(III) complexes with anionic ligands ($g_\parallel > g_\perp$).[14] The occurrence of these two distinct patterns is highly significant. It is interpreted as indicating (1) that there is a mixture of products, (2) that the mixture consists of a ligand-oxidized species and a low-spin nickel(III) species having a coordination number lower than six, and (3) that these two species probably exist in a thermal equilibrium. Each of these three points requires some additional comment.

The ligand-oxidized species is identified with the broad isotropic signals occurring around a g value of 2.00. It is reminiscent of the signals observed for the delocalized ligand radicals produced by one-electron oxidation of nickel porphyrins.[15-17] Consequently, this simple spectral feature is assigned to a structure in which the cyclidene ligand has been oxidized, producing a delocalized ligand radical, $[Ni^{II}(L^+\cdot)]^{3+}$.

The occurrence of a low-spin nickel(III) complex having a coordination number lower than six is inferred in the following way. The restrictive trimethylene bridge prevents the binding of solvent at one axial site. Reduction in the coordination number to five (or four) weakens the axial ligand field, and this may change the order of the metal d orbitals. Consequently, the unpaired electron may be in the d$_{xy}$ orbital, instead of the d$_{z^2}$ orbital, as is found among six-coordinated complexes suffering only weak axial distortions. Such a change in electronic structure can account for the inversion in the order of $g_\parallel$ and $g_\perp$ in going from unbridged $[NiL]^{3+}$, through the series of bridges of decreasing length, to the trimethylene bridged complex.

The presence of two distinct spectral patterns for the trimethylene derivative suggests a temperature-dependent equilibrium. Oxidized derivatives of nickel porphyrins have been reported to exhibit temperature-dependent changes between metal-centered- and ligand-centered-oxidation products. It is suggested that a similar thermal equilibrium occurs for the lacunar cyclidene complexes (eq 2).

$$[Ni^{III}(L)B]^{3+} \overset{\Delta}{\rightleftharpoons} [Ni^{II}(L^+\cdot)]^{3+} + B \qquad (2)$$
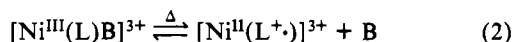
The ESR spectral behavior observed for the higher polymethylene-bridged complexes $[NiL]^{3+}$ at room temperature is

consistent with this model. These complexes exist, predominantly, as the ligand-oxidized species at these higher temperatures (Figure 6d). These same solutions, containing polymethylene-bridged nickel derivatives, display rather more complicated spectra at 77 K (Figure 6c), again indicating the possibility of mixtures of metal-centered- and ligand-centered-oxidation products.

Recapitulating, recalling that the oxidized form of the *unbridged* species contains six-coordinate nickel(III), it appears that the shorter polymethylene bridging groups restrict access to the metal ion and favor nickel(III) species having lower coordination numbers. This restriction on axial coordination limits the stabilization of the oxidized metal center with the result that both the ligand-centered- and the metal-centered-oxidation products exist at 77 K, in contrast to the unbridged species, which exists solely as the metal-oxidized species at this temperature.

Decreasing the ring size of the parent macrocycle has the effect of reducing the cavity size for a fixed bridging group. Thus, though it takes only an octamethylene group to produce six-coordinate nickel(III) in the case of the 16-membered macrocycle (16L), the decamethylene bridge is not adequate to permit strong axial ligation in the case of the 15-membered macrocycle. The ESR spectrum of $[Ni(15L)]^{3+}$ for $R^1 = (CH_2)_{10}$ corresponds to the case where the unpaired electron resides in d$_{xy}$ (i.e. $g_\parallel > g_\perp$, with no superhyperfine splitting). As pointed out by Riley,[20] decreasing parent macrocyclic ring size is accompanied by flattening of the saddle conformation of ligands related in structure to the cyclidenes. It follows that relatively long chains are required to provide cavities adequate to accept solvent in the case of $[Ni(15L)]^{3+}$. Simultaneously, the in-plane ligand field strength increases as the ring size decreases (given that the metal ion remains within the plane of the four donor atoms).[12,21] The combination of the two effects may drive d$_{xy}$ to higher energy than d$_{z^2}$ for the 15-membered ring derivative. At room temperature, the ESR spectrum due to the octamethylene-bridged $[Ni(15L)]^{3+}$ species clearly shows a ligand radical signal, in contrast to the ambiguous spectrum obtained for $[Ni(16L)]^{3+}$ under the same conditions. This is consistent with the expectation that the equilibrium shown in eq 2 should be shifted more to the right in the absence of strong axial ligation.

In summary, one readily visualizes three situations for the various oxidized cyclidene derivatives of nickel. The first, exemplified by the unbridged complexes, involves simple six-coordination of the trivalent nickel in the oxidized species, $[Ni^{III}L(An)_2]^{3+}$. In this case, the axial acetonitrile ligands are coordinated in the usual vertical fashion and this occurs only in the open, unbridged structure or with the least restrictive of bridges and most commodious of cavities. The contrasting extreme occurs with the most restrictive of bridges and involves a reduced coordination number of five (or four) for the nickel(III) complex. An intermediate case is also recognized. This occurs for bridges that are restrictive toward incoming ligands but not prohibitive, e.g. the pentamethylene and hexamethylene cases. The intermediate situation presumably permits coordination by a sixth ligand, under the bridge, but the metal ligand link for this ligand is weakened by the bridge. This model has been derived from studies on the ESR spectra of the complexes, but it is also consistent with the results of studies on their electronic absorption spectra.

Electronic Absorption Spectra of $[NiL]^{3+}$. The oxidized nickel cyclidene complexes show remarkable color properties, and these aid substantially in the elucidation of the structural relationships among these unusual complexes. The divalent nickel derivatives, $[Ni^{II}L]^{2+}$, are yellow in acetonitrile solution in the presence of 0.1 M (TBA)BF$_4$ supporting electrolyte, but the solutions of the oxidized species, $[NiL]^{3+}$, are highly colored. At room temperature, corresponding solutions of the oxidized species $[NiL]^{3+}$ having large lacuna appear deep green while those having in-

(13) Bencini, A.; Fabbrizzi, L.; Poggi, A. *Inorg. Chem.* **1981**, *20*, 2544.
(14) Lovecchio, F. V.; Gore, E. S.; Busch, D. H. *J. Am. Chem. Soc.* **1974**, *96*, 3109.
(15) Wolberg, A.; Manassen, T. *J. Am. Chem. Soc.* **1970**, *92*, 2982.
(16) Dolphin, D.; Niem, T.; Felton, R. H.; Fujita, I. *J. Am. Chem. Soc.* **1975**, *97*, 5288.
(17) Chang, D.; Malinski, T.; Ulman, A.; Kadish, K. M. *Inorg. Chem.* **1984**, *23*, 817.
(18) Wolberg, A.; Manassen, J. *Inorg. Chem.* **1970**, *9*, 2365.
(19) Johnson, E. C.; Niem, T.; Dolphin, D. *Can. J. Chem.* **1978**, *56*, 1381.

(20) Riley, D. P.; Stone, J. A.; Busch, D. H. *J. Am. Chem. Soc.* **1977**, *99*, 767.
(21) Busch, D. H.; Pillsbury, D. G.; Lovecchio, F. V.; Tait, A. M.; Hung, Y.; Jackels, S. C.; Rakowski, M. C.; Schammel, W. P.; Martin, L. Y. *ACS Symp. Ser.* **1977**, *No. 38*, 32.
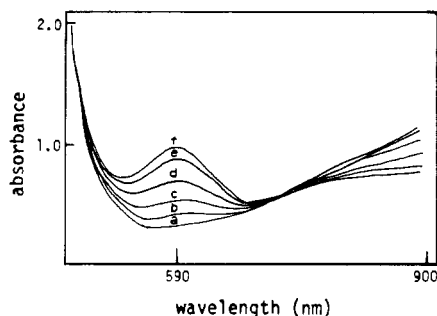
Figure 7. Temperature dependence of visible spectra of 2 mM unbridged [Ni(16L)]$^{3+}$ obtained by 1-e oxidative electrolysis of [Ni(16L)]$^{2+}$ at +0.90 V (vs. Ag/AgNO$_3$ 0.1 M) in acetonitrile, under nitrogen, 0.1 M (TBA)BF$_4$: (a) 247 K; (b) 255 K; (c) 265 K; (d) 274 K; (e) 285 K; (f) 292 K.

termediate or smaller lacuna are deep Prussian blue. The ultraviolet spectra of the oxidized complexes show little sensitivity to structure or temperature.

The electronic spectrum of the unbridged complex (R^1 = R^2 = R^3 = CH$_3$) shows a remarkable thermochromism that is particularly revealing (Figure 7). At 292 K an absorption band is observed at 590 nm for which an extinction coefficient of 400 cm^3 mol^{-1} cm^{-1} is estimated on the basis of total nickel content. As the temperature is lowered, the intensity of this band decreases until it is completely absent from spectra measured at 247 K. The process is totally reversible.

Since the 590-nm band is absent from the low-temperature spectrum and the low-temperature species has been unambiguously identified as a low-spin six-coordinate nickel(III) complex, this low-energy electronic transition must be typical of the ligand-oxidized species [Ni(L$^+$·)]$^{3+}$. Similar temperature-dependent spectral changes are observed for other [NiL]$^{3+}$ species having large lacuna.

The complexes having shorter polymethylene chains all display the high-intensity, low-energy absorption band in the region from 575 to 590 nm in their room-temperature spectra. Futher, the 590-nm band shows only small changes as the temperature is changed up to 248 K. These observations confirm the suggestion that the ligand-oxidized complex, [Ni^{II}(L$^+$·)]$^{3+}$, is the predominant species under these conditions.

The dependence of the electronic spectra of [NiL]$^{3+}$ on temperature and bridging group is consistent with our conclusion that equilibrium represented in eq 2 is governed by temperature and the extent of axial coordination. In those cases where both axial sites are available to coordination, the binding of two solvent molecules stabilizes the nickel(III) at low temperatures. When both sites are not fully available for coordination, the ideal six-coordinate nickel(III) cannot be formed and the equilibrium favors the ligand-oxidized species [Ni^{II}(L$^+$·)]$^{3+}$ At higher temperatures, even the unbridged species is at least partially converted to such a ligand-oxidized species.

Electronic Absorption Spectra of [CoL]$^{3+}$. The oxidized cobalt complexes [CoL]$^{3+}$ were generated electrochemically inside the dry nitrogen, controlled atmosphere in both acetonitrile and acetone solutions, in the presence of 0.1 M (TBA)BF$_4$ supporting electrolyte. Table II summarizes the data obtained on acetonitrile solutions, including the [ML]$^{2+/3+}$ oxidation potentials, the potentials applied for electrolysis, and the coulometric data. The oxidation potentials obtained from studies on acetone solutions are reported in Table IV. In order to generate the oxidized cobalt species, potentials 200 mV more positive than the half-wave potentials were applied.

A clear parallel is found between the electronic spectral behavior of the oxidized cobalt complexes and that described for nickel above. At room temperature, in acetonitrile solutions, and under a dry nitrogen atmosphere, the [CoL]$^{3+}$ complexes having short polymethylene bridges (trimethylene to pentamethylene) are green and exhibit a high-intensity absorption maximum at approximately 700 nm (Figure 8). In analogy to the nickel systems, this band is assigned to the presence of ligand-oxidized species that are

Table III. ESR Parameters[a] of the [Ni(L)]$^{3+}$ Lacunar and Related Unbridged Complexes

structure[f]	R^1	$g_{\parallel}$	$g_\perp$	g^e
I	(CH$_3$)$_2$	2.01	2.26	
I	(CH$_2$)$_8$	2.01	2.25	[b]
I	(CH$_2$)$_7$	2.25	2.07[c]	2.02
I	(CH$_2$)$_6$	2.25[d]	2.07[c]	2.02
I	(CH$_2$)$_4$	2.46	2.21	2.03
I	(CH$_2$)$_3$	2.46	2.21	2.03
II	(CH$_2$)$_8$	2.20	2.01	
II	(CH$_2$)$_{12}$	2.13[g]	2.03[g]	2.00[g]
I	(CH$_2$)$_{12}$	2.18	2.01	2.25[h]

[a] DPPH standard g = 2.0037. At 77 K, R^3 = R^2 = CH$_3$, and R^1 (bridge) is varied. [b] An additional feature of unclear origin is observed at g = 2.16 [c] Measured at the top of the shoulder. [d] There appears to be another signal of relatively low intensity at g = 2.35, which may be due to a five-coordinate complex similar to the one observed in the complexes with shorter bridges. [e] Inferred not to be part of the Ni(III) signal but that of [Ni^{II}S(L$^+$·)]$^{3+}$. Exceptions are (CH$_2$)$_{12}$-bridged complexes, see footnotes g and h below. [f] I = 16-membered and II = 15-membered macrocyclic tetradentate ligands. [g] Rhombic spectrum, $g_{xx} \neq g_{yy} \neq g_{zz}$. [h] Broad feature, may have two components.

Table IV. Effective Magnetic Moments of [Co(L)]$^{3+}$ (Structure I) and the Half-Wave Potentials of the 2+/3+ Redox Couples of Lacunar Complexes in Different Solvents[a]

	solvent			
	acetone		acetonitrile	
R^1	μ_{eff}, μ_B	$E_{1/2}$,[b] V	μ_{eff}, μ_B	$E_{1/2}$, V
(CH$_3$)$_2$	[d]	0.02	[c]	-0.15
(CH$_2$)$_6$	3.0	0.27	[d]	0.20
(CH$_2$)$_5$	2.9	0.26	2.9	0.28
(CH$_2$)$_4$	2.9	0.28	2.7	0.34

[a] R^3 = R^2 = CH$_3$, R^1 is varied, and T = 300 ± 3 K. [b] In volts, with rotating Pt-disk working electrode, Ag/AgNO$_3$ (0.1 M) reference in acetonitrile, and 0.1 M (TBA)BF$_4$ electrolyte. [c] Diamagnetic. Does not react with oxygen. [d] Appears to be diamagnetic. Reacts with oxygen.
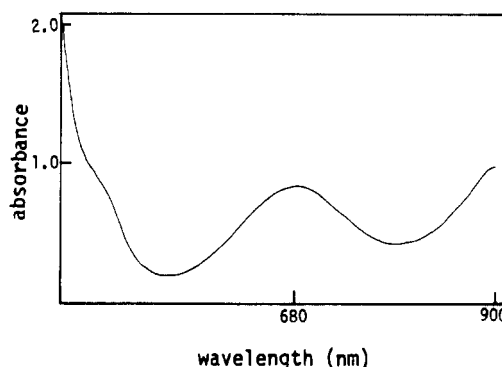
Figure 8. Visible spectrum of (CH$_2$)$_4$-bridged [Co(16L)]$^{3+}$ (R^3 = R^2 = CH$_3$) complex in acetonitrile with 0.1 M (TBA)BF$_4$ electrolyte, at room temperature under nitrogen.

formed because formation of a stable six-coordinate cobalt(III) complex is prevented by the restrictive bridge. For intermediate or large lacuna, R^1 = (CH$_2$)$_{6,7,8}$ or (CH$_3$)$_2$, no such spectral feature is observed and the solutions are brown. The latter species are all presumed to be genuine cobalt(III) complexes, and this is borne out by magnetic measurements (vide infra).

The most striking difference in behavior between the oxidized cobalt and oxidized nickel complexes, as studied in acetonitrile solutions, is the obvious more dominant apperance of stable trivalent species in the cobalt case. The great tendency of the low-spin d^6 cobalt(III) species to assume the coordination number of six may well permit that ion to bind ligands under less favorable conditions than is possible for the axially distorted low-spin d^7 nickel(III) ion.

The contrasting observations made on solutions of [CoL]$^{3+}$ in acetone solutions support the view that the effects reported above

are indeed dependent on coordination of the solvent. Acetone is a very weak ligand toward such metal ions as cobalt(III). The acetone solutions of all of the electrogenerated 16-membered cyclidene [CoL]³⁺ complexes, except the unbridged complex, are green and show absorption bands in the region around 700 nm. The exceptional behavior of the unbridged complex is considered later in this discussion.

Magnetic Moments of [CoL]³⁺. The cobalt(III) complexes are expected to be ESR silent because of the absence of unpaired electrons. On the other hand, the ligand-oxidized cobalt species [Co(L⁺·)]³⁺ could have two unpaired electrons, one on the ligand and one associated with low-spin cobalt(II). Wolberg and Manassen found that porphyrin complexes having similar electronic arrangements are ESR silent.[15] As these relationships predict, all attempts to detect ESR signals on the oxidized cobalt cyclidene complexes failed. Experiments were performed with R¹ = (C-H₂)₃,₄,₅ in acetonitrile and R¹ = (CH₂)₄,₆ and (CH₃)₂ in acetone solutions at 77 K.

Magnetic moments were determined for a number of the oxidized cobalt species in solution and are reported in Table IV. It is immediately clear that all combinations of complex and solvent that produce electronic absorption bands in the 700-nm region also produce magnetic moments consistent with the presence of two unpaired electrons, thereby confirming the structure as [Co^{II}(L⁺·)]³⁺. It is equally satisfying that the complexes to which cobalt(III) structures were assigned on the basis of electronic spectra show no unpaired spins in these magnetic moment determinations.

The magnetic moment of the tetramethylene-bridged species [CoL]³⁺ was measured over the temperature range from 235 to 290 K and found to be invariant. Paramagnetic cobalt(III) complexes have been claimed.[22-24] For example, a Schiff base complex was found to exhibit a temperature-dependent paramagnetism in the absence of strong nitrogenous axial bases while becoming diamagnetic in the presence of pyridine. Interestingly, a color change from green to brown accompanied this change in spin state.[23] In the present cases, the alternate explanation that the $S = 1$ state arises from an intermediate-spin cobalt(III) species is not very attractive. Given the large range of related structures and the consistent values observed for the magnetic moment, this would be most unusual. If changes between spin states of cobalt were involved, one would expect to observe mixtures of spin states and relatively random values of the magnetic moment at any given temperature. One might argue that the relative ease of oxidation of the cobalt complexes, compared to that of their nickel counterparts, even for the species having short bridges, supports the metal center as the locus of oxidation. This may well be true; however, the species we have characterized are the long-term products and do not necessarily reflect the locus of the initial electron-transfer event.

The unbridged complex [CoL]³⁺ presents the only apparent deviation from a perfectly understandable behavior among these cobalt species. It is considered surprising that this species is diamagnetic in acetone solution. We rationalize this on the assumption that traces of water in the solvent may provide the axial ligands necessary to stabilize cobalt(III) in this case. In this regard it is true that the hydrophobic character of the lacuna seems to consistenly prevent coordination of water within that cavity.

Reactions of Certain [CoL]³⁺ Species with Dioxygen. A most unusual reaction has been observed between these oxidized cobalt species and the dioxygen molecule. The obvious conclusion for such a process is that the proposed ligand radical is merely capturing the dioxygen radical, a very well-known reaction. The fascinating aspect of the phenomenon reported here is that this seems not to be the case.

Figure 9, parts a and b, shows cyclic voltammograms of the hexamethylene-bridged cobalt(II) species measured in 0.1 M

E (volts)
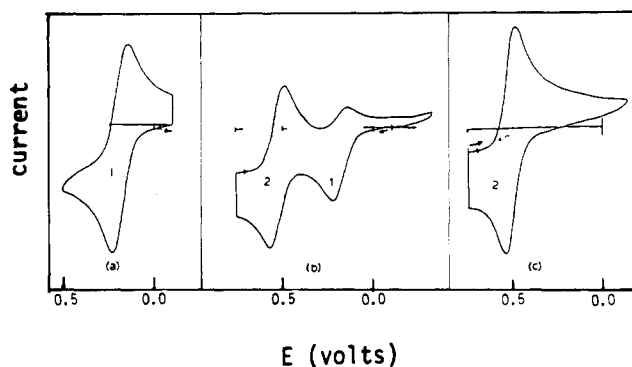
Figure 9. Cyclic voltammograms of the (CH₂)₆-bridged [Co(16L)]³⁺ species in acetonitrile (0.1 M (TBA)BF₄): (a) [Co(16L)]²⁺ under nitrogen; (b) [Co(16L)]²⁺ upon exposure to air; (c) ([Co(16L)]³⁺ solution exposed to dioxygen. Pt-wire working electrode, Ag/AgNO₃ (0.1 M) reference.

Table V. Comparison of the R¹-Dependent Reactivity of [Co(16L)]²⁺ and [Co(16L)]³⁺ in Acetonitrile with Dioxygen[a]

	reacts with dioxygen	
R¹	[Co(16L)]²⁺[b]	[Co(16L)]³⁺
(CH₂)₃	no	no
(CH₂)₄	no[c]	no
(CH₂)₅	yes	yes
(CH₂)₆	yes	yes
(CH₂)₇	yes	yes
(CH₃)₂[c]	yes	no[e]

[a]R² = R³ = CH₃. [b]Data obtained in the presence of excess N-methylimidazole. [c]Small binding constant measurable only at 233K.[8] [d]Unbridged complex. [e]Reacts in acetone solution.

(TBA)BF₄ acetonitrile under dry nitrogen (Figure 9a) and under dry air (Figure 9b). The new feature appearing upon exposure to air is the dominant feature in the experiment shown in Figure 9c. In this case, [CoL]³⁺ is electrogenerted inside the dry nitrogen atmosphere enclosure and then exposed to dioxygen and the cyclic voltammogram is taken. A new redox couple, about 300 mV more anodic than the original [CoL]²⁺⁰³⁺ wave, is observed upon exposure to dioxygen, and it is clearly due to a reaction of the [CoL]³⁺ species with dioxygen. Further, this reaction between [CoL]³⁺ (R¹ = (CH₂)₆) and dioxygen is irreversible. Similar though less well-defined reactions with dioxygen are found with a number of the other lacunar cyclidene complexes (Table V).

In a previous section the complex under discussion, [CoL]³⁺ (R¹ = (CH₂)₆), was found to contain diamagnetic cobalt(III) and, presumably, unaltered ligand. A stable six-coordinate cobalt(III) complex is not expected to react with dioxygen. However, because of the hindered coordination of the solvent molecule that must enter the lacuna, one can accept the possibility of an equilibrium of the sort given in eq 3, but favoring the diamagnetic form. Here,

$$[Co^{III}(L)AnAn']^{3+} \rightleftharpoons [Co^{II}(L⁺·)An]^{3+} + An \qquad (3)$$
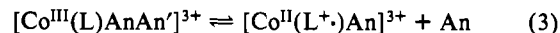
An' indicates an acetonitrile molecule that is coordinated within the cavity in a bent fashion.[25] The [Co^{II}(L⁺·)An]³⁺ complex on the right side of equilibrium 3 has two obvious avenues open for reaction with dioxygen. The ligand radical could capture dioxygen, or the cobalt(II) could complex with dioxygen. The possibility also exists that the dioxygen might interact with the cobalt(II) by coordination, outside the lacuna, below the plane of the macrocyclic donor atoms. In order for this to occur, the complex would have to exist, at least to some extent, in the four-coordinate form.

(22) Huet, J.; Gaudemer, A.; Boucly-Goester, C.; Boucly, P. *Inorg. Chem.* **1982**, *21*, 3413.
(23) Gerloch, M.; Higson, B. M.; McKenzie, E. D. *J. Chem. Soc., Chem. Commun.* **1971**, 1149.
(24) Goedken, V.; Peng, S.-M. *J. Chem. Soc., Chem. Commun.* **1975**, 258.

(25) The crystal structure of a bis(thiocyanato)-coordinated cobalt(III) lacunar complex in ref 3 shows an NCS ligand bound at the axial site inside the lacuna at an unusually bent angle. This demonstrates the steric hindrance due to the R¹ bridging group. Acetonitrile, by analogy, must bind at the axial site inside the lacunar complex in a similar bent fashion.

Table V shows the distinct selective reactivity with dioxygen that has been observed for the series of oxidized cobalt cyclidene complexes. For purposes of comparison, the table also indicates whether the parent cobalt(II) complexes form dioxygen adducts of the usual Pauling type. The selectivity observed places interesting limitations on the nature of this peculiar reaction.

It is found that [CoL]$^{3+}$ species that have small lacuna and that exist predominantly as ligand-oxidized species do NOT react with dioxygen. This rules out the possibility that dioxygen is reacting with the ligand radical. The possibility that the reaction involves four-coordinate cobalt can also be ruled out since reaction outside the lacuna should not depend on bridge length.

These considerations suggest (1) that dioxygen reacts with the small amount of [Co^{II}(L^{+}·)An]$^{3+}$ that exists in equilibrium with [Co^{III}(L)AnAn′]$^{3+}$ in the cases of those lacunar cyclidene complexes having intermediate and large cavities, (2) that the [Co^{II}(L^{+}·)An]$^{3+}$ complexes are five-coordinate with the unhindered axial site occupied by an acetonitrile molecule, and that (3) dioxygen coordinates to the cobalt(II) inside the lacuna. The nature of this product does, however, remain unclear.[26] It should be noted that the unbridged [CoL]$^{3+}$ complex is not reactive toward dioxygen in acetonitrile solution, but that it does undergo a similar reaction in acetone solution. This is expected since the unhindered binding to two axial acetonitrile ligands should stabilize cobalt(III), apparently in this case, to the exclusion of the equilibrium given in eq 3.

Summary. In this report, we have investigated the question of the site of oxidation in the cobalt and nickel complexes with the lacunar and unbridged cyclidene ligands. These ligands form important families of cobalt and iron complexes that bind dioxygen with exceptional facility and flexibility. Whether it is the metal center or some part of the ligand system that provides the electron for oxidation is a matter of significance in the management of dioxygen chemistry by transition-metal complexes. We have shown that the cobalt(II) and nickel(II) complexes with different polymethylene bridging groups can be oxidized by a one-electron process to produce different oxidation products, depending on the following factors: (1) Small lacunae inhibit the formation of six-coordinate complexes and favor the formation of species in which the ligand has been oxidized, [Ni^{II}(L^{+}·)]$^{3+}$ and [Co^{II}-(L^{+}·)]$^{3+}$; large lacunae permit binding of two axial ligands, which stabilizes complexes containing the trivalent metal ions, [Ni^{III}-(L)An$_2$]$^{3+}$ and [Co^{III}(L)An$_2$]$^{3+}$. (2) Strong axial ligands favor the trivalent derivative; i.e., in the case of the hexamethylene bridge, [Co^{III}(L)AnAn′]$^{3+}$ exists in acetonitrile but [Co^{II}(L^{+}·)]$^{3+}$ exists in acetone. (3) Higher temperatures favor the ligand-oxidized species, possibly by labilizing the axial ligands.

The several relationships described above confer kinetic complications on the overall 2+/3+ redox reactions. The difference in the potentials for the first oxidation processes of the tetramethylene-bridged complex and for the unbridged cobalt cyclidene complex is clearly due to the destabilization of the cobalt(III) state. However, the fact that such a large difference in the corresponding potentials is not observed for the nickel complexes suggests that the two redox reactions are quite different. We shall be dealing with the mechanisms of the redox reactions and their effect on the observed potentials in a separate paper.[9]

Experimental Section

Solvents and Reagents. Reagent grade acetonitrile was allowed to stand over calcium hydride (about 5 g of calcium hydride/L of acetonitrile) for several days and stirred overnight just prior to distillation. The mixture was refluxed for about 2 h and distilled under a nitrogen atmosphere. The collected distillate was deoxygenated by bubbling nitrogen through it for about 15 min. The deoxygenated solvent was stored inside the dry nitrogen atmosphere enclosure.

Reagent grade acetone was stirred over 4-Å molecular sieves for 7–10 days and allowed to stand for a few additional days. Acetone was decanted quickly into a flask containing potassium permanganate (about 2 g/L), refluxed for about 1 h, and distilled under nitrogen. When the distillate was cloudy, it was redistilled until clear. Acetone was degassed in a manner identical with that used for acetonitrile, as described above. The solvent was stored inside the dry nitrogen atmosphere glovebox.

Compounds and Reagents. Tetra-*n*-butylammonium tetrafluoroborate was purchased from the Southwestern Analytical Co. The nickel and cobalt complexes used in this study were synthesized according to procedures published elsewhere[1-3,8] and were donated by colleagues in the research group of Professor Busch or synthsized by M.Y.C. We are grateful for the generosity of our colleagues.

Physical Measurements. Electrochemical measurements were performed with Princeton Applied Research Corp. instrumentation: a Model 173 potentiostat/galvanostat, a model 175 linear programmer, and a Model 179 digital coulometer. Cyclic voltammetric curves were recorded on Houston Instruments 2000 or Hewlett-Packard/Mosley Division XY recorders. All solutions for electrochemical experiments were prepared inside the dry nitrogen atmosphere enclosure by using dry deoxygenated solvents and 0.1 M N-tetrabutylammonium tetrafluoroborate supporting electrolyte. A platinum-disk working electrode, platinum-wire auxiliary electrode, and Ag/AgNO$_3$ (0.1 M) reference electrode were used in a two-compartment H cell for cyclic voltammetric studies, within the dry nitrogen atmosphere enclosure. The working electrodes were cleaned with the dry distilled solvent that was to be used in a given experiment. Background curves were recorded prior to making CV measurements.

For coulometric experiments, three-compartment cells with a Ag/AgNO$_3$ (0.1 M) reference electrode and a platinum-gauze working electrode were used. The sample was placed in the working-electrode compartment, stirring was begun (stir bar), and the electrolysis was then initiated. The process was stopped when the current had dropped to about 1% of its initial value. The potentials used were about 200 mV more anodic than the half-wave potentials for the processes in question, as determined by cyclic voltammetry. Solutions prepared in this way were used for ESR and UV–visible spectroscopy and for magnetic moment determinations. Care was taken to remove solutions from the working-electrode compartment without allowing mixing with the solution from the auxiliary electrode compartment.

ESR spectra were obtained with a Varian Model 102 ESR spectrometer. They were determined on frozen glasses at liquid-nitrogen temperature, by using tubular quartz cells and, for room-temperature measurements, a flat quartz cell with a capillary tip (Wilmad Glass Co. WG-814). Signal assignment was made relative to a (DPPH) pitch sample with g = 2.0037.

UV–visible spectra were recorded by using a Cary Model 17D spectrophotometer having an arrangement for thermostating the cell compartment. The sample was contained in a quartz cuvette with the cap sealed by vacuum grease.

The magnetic moments were measured by the Evans method,[27] using ^{1}H NMR spectra recorded with a Bruker WM300 (300MHz) spectrometer. The deuterated solvents (99%), Aldrich Gold Label) were used upon deoxygenation by bubbling nitrogen and were not dried or subjected to purification.

Registry No. I (M = Ni^{II}, R^1 = (CH$_3$)$_2$, R^2 = R^3 = CH$_3$), 99685-52-6; I (M = Ni^{III}, R^1 = (CH$_3$)$_2$, R^2 = R^3 = CH$_3$), 99656-53-8; I (M = Ni^{II}, R^1 = (CH$_2$)$_{12}$, R^2 = R^3 = CH$_3$), 99656-43-6; I (M = Ni^{III}, R^1 = (CH$_2$)$_{12}$, R^2 = R^3 = CH$_3$), 99656-54-9; I (M = Ni^{II}, R^1 = (CH$_2$)$_8$, R^2 = R^3 = CH$_3$), 76791-40-7; I (M = Ni^{III}, R^1 = (CH$_2$)$_8$, R^2 = R^3 = CH$_3$), 99656-55-0; I (M = Ni^{II}, R^1 = (CH$_2$)$_7$, R^2 = R^3 = CH$_3$), 76791-36-1; I (M = Ni^{III}, R^1 = (CH$_2$)$_7$, R^2 = R^3 = CH$_3$), 99656-56-1; I (M = Ni^{II}, R^1 = (CH$_2$)$_6$, R^2 = R^3 = CH$_3$), 73914-15-5; I (M = Ni^{III}, R^1 = (CH$_2$)$_6$, R^2 = R^3 = CH$_3$), 99656-57-2; I (M = Ni^{II}, R^1 = (CH$_2$)$_5$, R^2 = R^3 = CH$_3$), 76791-38-3; I (M = Ni^{III}, R^1 = (CH$_2$)$_5$, R^2 = R^3 = CH$_3$), 99656-58-3; I (M = Ni^{II}, R^1 = (CH$_2$)$_4$, R^2 = R^3 = CH$_3$), 76800-63-0; I (M = Ni^{III}, R^1 = (CH$_2$)$_4$, R^2 = R^3 = CH$_3$), 99656-59-4; I (M = Ni^{II}, R^1 = (CH$_2$)$_3$, R^2 = R^3 = CH$_3$), 93366-18-8; I (M = Ni^{III}, R^1 = (CH$_2$)$_3$, R^2 = R^3 = CH$_3$), 99656-60-7; I (M = Co^{II}, R^1 = (CH$_3$)$_2$,

(26) A one-electron controlled-potential oxidative electrolysis of the complex generated by the irreversible reaction between O$_2$ and [Co^{II}(L^{+}·)]$^{3+}$ in acetonitrile generated a magenta solution with a high-intensity visible absorption band at ca. 540 nm. This solution gave an isotropic ESR signal at g = 2.00 with 30–32 equally spaced hyperfine lines (A = 5.76 G) at room temperature. ESR studies using ^{17}O-enriched dioxygen suggest that O$_2$ is present in this complex.

(27) Evans, D. F. *J. Chem. Soc.* **1959**, 2003.

Contribution from the Dipartimento di Chimica Generale, Università di Pavia, 27100 Pavia, Italy, and Institut für Anorganische Chemie, Universität Basel, 4056 Basel, Switzerland

Complexation of Divalent and Trivalent Nickel and Copper Ions by Rigid and Flexible Dioxo Tetraaza Macrocycles

Luigi Fabbrizzi,*[1a] Thomas A. Kaden,*[1b] Angelo Perotti,[1a] Barbara Seghi,[1a] and Liselotte Siegfried[1b]

Received July 2, 1985

Potentiometric, spectrophotometric, kinetic, and electrochemical studies on the Ni^{2+} and Cu^{2+} complexes with the two macrocycles **1** and **2** have been performed to investigate the importance of the flexibility of the macrocyclic ring to the properties of the corresponding complexes. The more flexible ligand **1** gives a series of Cu^{2+} complexes with variable protonation stoichiometry, whereas ligand **2** only forms a Cu^{2+} complex of the type [CuLH$_{-2}$]. The two ligands also differ in their complexation kinetics, the reactivity of **1** being higher than that of **2**. Thus from its equilibria and kinetics, ligand **1** closely resembles open-chain ligands, whereas the reactivity of **2** is typical for macrocycles. On the other hand, the redox potential of the M(III)/M(II) couple is practically independent of the rigidity of the macrocyclic ring.

Introduction

The study of metal complexes with tetraaza macrocycles has been developed from the thermodynamic[2] as well as from the kinetic point of view.[3] With the report of the synthesis of dioxo tetraaza macrocycles by Tabushi et al.[4] and the complexation studies of these ligands with Ni^{2+} and Cu^{2+} by Kimura et al.,[5,6] new and interesting properties of these macrocycles have been observed. So dioxo tetraaza macrocycles (a) can coordinate Ni^{2+} and Cu^{2+} with dissociation of two protons from the amido groups,[5,6] giving neutral complexes MLH$_{-2}$, (b) exhibit dissociation kinetics that are relatively fast compared to those of the analogous tetraamine macrocyclic compelxes,[7] and (c) form Ni^{2+} and Cu^{2+} complexes that can be electrochemically oxidized to give trivalent species, sometimes stable even in aqueous solution.[6,8,9]

Most of the dioxo macrocycles studied up to now have two amide groups cis to each other (ligands **3** and **4**). These ligands have the advantage of a relatively rigid structure when the two amide groups are deprotonated and thus produce strong ligand fields.

However, there are in the literature also a few dioxo macrocycles with trans amide groups, such as ligands **1** and **2**, and their complexation properties have only partially been studied.
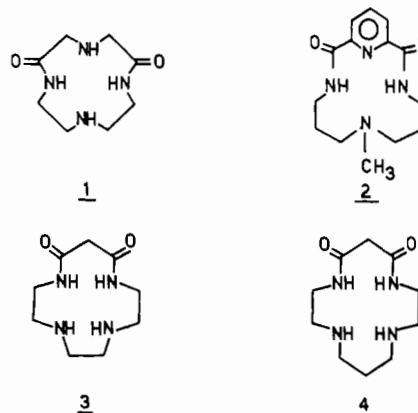
We report here a series of equilibrium measurements, the kinetics of formation and dissociation of their Ni^{2+} and Cu^{2+}

(1) (a) Università di Pavia. (b) Universität Basel.
(2) Fabbrizzi, L.; Micheloni, M.; Paoletti, P. *Inorg. Chem.* **1980**, *19*, 535–538.
(3) Leugger, A.; Hertli, L.; Kaden, Th. A. *Helv. Chim. Acta* **1978**, *61*, 2296–2306.
(4) Tabushi, I.; Taniguchi, Y.; Kato, H. *Tetrahedron Lett.* **1977**, *18*, 1049–1052.
(5) Kodama, M.; Kimura, E. *J. Chem. Soc., Dalton Trans.* **1979**, 325–329.
(6) Kodama, M.; Kimura, E. *J. Chem. Soc., Dalton Trans.* **1981**, 694–700.
(7) Hay, R. W.; Pujari, M. P.; McLaren, F. *Inorg. Chem.* **1984**, *23*, 3033–3035.
(8) Fabbrizzi, L.; Poggi, A. *J. Chem. Soc., Chem. Commun.* **1980**, 646–647.
(9) Fabbrizzi, L.; Perotti, A.; Poggi, A. *Inorg. Chem.* **1983**, *22*, 1411–1412.